

Extending Femtosecond Metrology to Longer, More Complex Laser Pulses in Time and Space

Jacob Cohen, Pamela Bowlan, and Rick Trebino, *Member, IEEE*

(Invited Paper)

Abstract—We review several recently developed simple, yet powerful, techniques for the measurement of the complete temporal (and spatiotemporal) intensity and phase of laser pulses up to nanoseconds in length. Spatially encoded arrangement for temporal analysis by dispersing a pair of light e-fields (SEA TADPOLE) is a simple and practical variation of spectral interferometry that can measure pulses as long as ~ 50 ps with complexities, that is, time-bandwidth products (TBPs) as large as ~ 100 . SEA TADPOLE can also measure the complete spatiotemporal electric field of pulses with femtosecond temporal and submicrometer spatial resolution. Using a train of identical reference pulses, multiple delays for temporal analysis by dispersing a pair of light e-fields (MUD TADPOLE) extends SEA TADPOLE to pulses up to several nanoseconds long with TBPs of $\sim 100\,000$ or more. Finally, a simple variation of frequency-resolved optical gating (FROG) measures the complete intensity and phase of nanosecond-long laser pulses on a single shot without a reference pulse. It uses a novel approach in which the pulse to be measured is tilted by $\sim 89.9^\circ$, so that one side of it precedes the other by over a meter, yielding several nanoseconds of delay without appreciably distorting the pulse in time. This remarkably simple and compact FROG device has no sensitive alignment parameters.

Index Terms—Laser amplifiers, optical pulse measurement, pulse generation, pulsed lasers.

I. INTRODUCTION

FEMTOSECOND (fs) light pulses are now arguably the best characterized type of light—even better than continuous wave (cw) light, which still requires a statistical description. This is actually not surprising because the measurement of an ultrashort laser pulse requires easily generated delays of micrometers to at most a few centimeters and easily attained spectral resolutions of nanometers (nm). As a result, ultrafast metrology has rapidly evolved from a few rudimentary (and often difficult to perform) techniques to some of the most sophisticated and elegant optical techniques currently in use. And perhaps as a

result, ultrafast lasers are now also the most stable lasers in the world, a fact that has significantly contributed to advances in ultrafast chemistry and frequency combs, two fields that have recently earned Nobel prizes.

The first devices used to measure pulsed lasers were simple light detectors with oscilloscopes for readout. At the time (the 1960s), these devices were fast enough to characterize the intensity versus time of the many-nanosecond (ns)-to-microsecond (μ s) pulses that were the state of the art at the time. The pulse phase went unmeasured, however.

As researchers generated ever shorter pulses, ns and later ps long, laser users quickly realized the need for faster measurement techniques. Fortunately, autocorrelation techniques emerged, which involved splitting the pulse into two replicas, varying their relative delay, crossing them in a nonlinear-optical medium, and measuring the nonlinear-optical signal-pulse energy versus delay. This yielded a rough measure of the pulse length [1], [2]. But retrieving the intensity versus time from an autocorrelation is equivalent to the 1-D phase-retrieval problem—a highly ill-posed problem. This meant that autocorrelation gave little quantitative information, especially for complex pulses, for which it yielded only the sum of a broad washed-out background and a narrow coherence artifact. Worse, the autocorrelation also said nothing about the pulse phase, which was necessary for a complete measurement of the pulse. In the 1980s, an interferometric version of autocorrelation was introduced, but it only yielded qualitative information about the phase and, like its noninterferometric cousin, failed badly for complex pulses. Because pulse structure washes out in both types of autocorrelation, later attempts to combine it with an independent measurement of the spectrum [3] similarly have failed to uniquely determine either the intensity or the phase of the pulse.

It was not until pulses reached fs lengths that complete temporal-intensity-and-phase measurements became possible. In 1991, the first such technique, frequency-resolved optical gating [4] (FROG), a simple spectrally resolved autocorrelation with a well-posed 2-D phase-retrieval algorithm, was introduced. FROG is actually a broad class of methods that measure pulses of different wavelengths, durations, and complexities for a wide array of ultrafast measurement problems, including the measurement of attosecond (as) pulses. In the succeeding years, FROG has been significantly simplified, [4] and additional alternative methods have also been developed.

While spectacular progress has occurred over the last two decades in the measurement of ~ 100 as to ~ 50 ps pulses, progress in the measurement of pulses with durations in the range of ~ 50 ps to 10 ns has lagged behind. At first glance

Manuscript received October 14, 2010; revised November 7, 2010 and November 29, 2010; accepted December 16, 2010. Date of publication April 5, 2011; date of current version January 31, 2012. This work was supported in part by the Defense Advanced Research Projects Agency under Grant FA8650-09-C-9733.

J. Cohen is with ASML, Eindhoven, The Netherlands (e-mail: jcohen7@gatech.edu).

P. Bowlan is with the Max-Born-Institute, 12489 Berlin, Germany (e-mail: pambowlan@gmail.com).

R. Trebino is with the Georgia Institute of Technology, Atlanta, GA 30332 USA (e-mail: rick.trebino@physics.gatech.edu).

Color versions of one or more of the figures in this paper are available online at <http://ieeexplore.ieee.org>.

Digital Object Identifier 10.1109/JSTQE.2011.2107314

this seems surprising, as slower events ought to be easier to measure. But such pulses actually require a much more difficult combination of very high spectral resolution [picometer (pm)] and/or very large delays (meters). Perhaps also, the measurement of such longer pulses has been considered less exciting than that of more exotic fs and as pulses. However, ns lasers far outnumber fs and ps lasers and have many more applications. Furthermore, ns lasers are arguably the *least stable* lasers in the world, often having time-bandwidth products (TBPs—a measure of pulse complexity) in the hundreds and exhibiting massive fluctuations in their pulse shapes and energies from shot to shot. It is probably not a coincidence that they are also arguably the most poorly measured pulses.

Further complicating the ns-pulse measurement problem are the fields of pulse shaping and arbitrary-optical-waveform generation, whose purpose is to deliberately generate extremely complex pulses. In the latter case, the goal is a pulse length of ~ 10 ns with ~ 100 -fs temporal structure, yielding a TBP of $\sim 100\,000$. Such incredibly complex pulses require new measurement techniques with unprecedented power.

As a result, ns pulses require two classes of measurement techniques, first a self-referenced technique for completely measuring potentially complex ns pulses directly from (potentially unstable) lasers and hence without the benefit of a reference pulse. And second, because arbitrary optical waveforms and shaped pulses in general are made from simple ultrashort pulses that are easily measured using available techniques, a class of techniques is also needed that can take advantage of a readily available reference pulse and that can measure extremely complex pulses. And ideally, each would operate on a single shot and not require averaging over many identical pulses.

Researchers have made progress extending ultrafast measurement techniques to the ps regime and to more complex pulses. For example, FROG, in its multishot variation, has been used to measure pulses up to 80 ps in length [5], and FROG measurements have been made with 20-ps temporal range and sub-ps temporal resolution [6]–[8]. And we have recently developed a simple version of FROG [grating-eliminated no-nonsense observation of ultrafast incident laser light e-fields (GRENOUILLE)] with only three easily aligned optical elements that can measure single pulses up to ~ 20 ps long with TBPs of up to ~ 20 [9].

FROG, in its cross-correlation FROG (XFROG) variation, has been used to measure pulses with TBPs of several thousand [10], but only for pulses several ps long. And although the FROG-retrieval algorithm is rather fast for pulses with TBPs < 10 , retrievals of complex pulses with TBPs > 1000 can take more than an hour on a standard desktop computer, and therefore, it is difficult to imagine measuring significantly more complex pulses using it, especially on a single shot.

Additionally, several time-domain techniques based on temporal imaging can measure at least the temporal intensity of ps pulses [11], [12] by stretching them to many ns in length, where detectors and oscilloscopes can accurately measure their intensities versus time. In addition, high-bandwidth oscilloscopes and streak cameras have improved and can themselves also measure the temporal intensity of ps and ns pulses. Heterodyning with a delayed version of the pulse or with another known pulse can

yield the phase. Several techniques use this approach, including a variety of additional processes, such as four-wave mixing in fibers [13]. Alternatively, Vampouille *et al.* introduced [14] and Ippen and coworkers have recently utilized a ns-pulse streak-camera-and-monochromator-based technique that generates a sonogram [15]. The sonogram is mathematically equivalent to the spectrogram [4] and is capable of yielding the full pulse electric field. However, all of these techniques involve a complex apparatus and/or expensive and fragile electronics.

In addition, a number of linear self-referencing techniques use very high bandwidth temporal modulators to measure pulses ~ 100 ps long with high sensitivity [16], [17]. However, these techniques require precise electronic synchronization of the pulse under test with the temporal modulator and so are difficult to use and are typically only useful for trains of identical pulses.

In short, most \sim ns pulses go unmeasured, so it is reasonable to conclude that sufficiently convenient and powerful techniques for their measurement have not yet been developed.

One very simple technique with the potential to measure both ns-long and very complex pulses is spectral interferometry (SI) [18]. In its simplest form, SI involves measuring the spectrum of the sum of two pulse fields, that of a reference pulse and an unknown pulse. The result is a spectral interferogram from which both the spectral intensity and the phase of the unknown pulse can be retrieved. SI is inherently a single-shot technique, and the interferogram can be directly and quickly inverted regardless of the complexity of the pulse. Another useful property of SI is that it is a linear-optical technique, and so it is extremely sensitive and can measure pulses that are approximately nine orders of magnitude weaker than those that can be measured using nonlinear-optical methods [19]. SI's only fundamental drawback is that it requires a previously measured reference pulse whose spectrum contains that of the unknown pulse. Fortunately, when measuring shaped pulses and arbitrary waveforms, the unshaped pulse provides an ideal such reference pulse, and it is easily measured using another technique, such as FROG or its experimentally simpler version, GRENOUILLE.

Unfortunately, the most common version of SI, Fourier transform SI (FTSI), has two rather severe practical limitations that have prevented it from measuring such pulses. First, the filtering algorithm used to reconstruct the unknown pulse from the spectral interferogram requires that the reference and unknown pulses be separated in time and so reduces the spectral resolution of the device by about factor of 5. Second, it has extremely strict alignment requirements, such as perfectly collinear beams with similar intensities and identical spatial modes, so its alignment is difficult and it must be frequently readjusted.

To overcome these limitations, there have been a number of advances resulting in the measurement of more complex waveforms [20]–[23]. But, even with these improvements, these methods are limited either by the spectral resolution of the spectrometer [24] or by the temporal resolution of a photodetector. And they remain very difficult to align and maintain aligned.

Here, we review three powerful new techniques that we have recently developed, which extend SI and FROG to measure the complete electric field of both extremely complex shaped

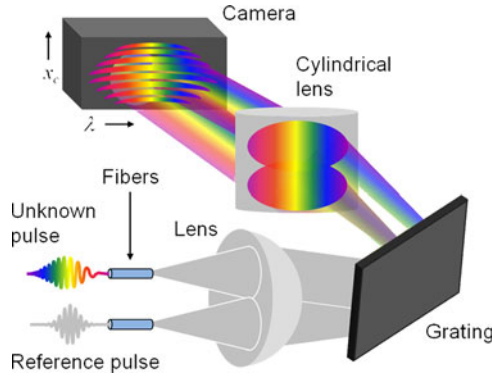


Fig. 1. Experimental setup for SEA TADPOLE: the reference and unknown pulses enter the device via equal-length, single-mode optical fibers. In the horizontal dimension, the light is collimated and then spectrally resolved at the camera using the grating and the cylindrical lens. In the vertical dimension, the light emerging from the two fibers crosses at a small angle causing horizontal spatial fringes at the charge-coupled device camera.

pulses—in time and also in space—and ns pulses directly from laser sources (in time and without a reference pulse).

II. MEASURING SHAPED PULSES: SEA TADPOLE

We recently introduced a single-shot linear spectral interferometer that solves the alignment and spectral-resolution reduction problems of FTSI and, as a result, is capable of measuring complex shaped pulses easily. It is called spatially encoded arrangement for temporal analysis by dispersing a pair of light E-fields (SEA TADPOLE) (see Fig. 1) [20], [25]–[27]. It involves crossing at an angle the pulse to be measured with a previously measured reference pulse. The crossed beams generate a *spatial* interferogram, from which the unknown pulse’s intensity and phase can be *spatially* (rather than spectrally) filtered without loss of spectral resolution, and which greatly reduces the alignment burden commonly associated with SI. Additionally, SEA TADPOLE uses optical fibers (which can be overfilled by the beam) as inputs for both the reference and unknown pulses, significantly simplifying its alignment and providing high spatial resolution, if desired. And it should be mentioned that the dispersion introduced by the identical-length fibers cancels out, so they introduce no distortions in the measurement.

In the SEA TADPOLE experimental setup illustrated in Fig. 1, the output ends of the fibers are placed close together, so that when the light diverges from them, both beams are collimated by the same spherical lens, located a focal length f away from the fibers. Because the fibers are displaced from the optic axis (with a distance d between them, which is usually ~ 1 mm), the collimated beams cross at an angle $\theta \approx d/f$, and a camera at the crossing point records their interference. In the other dimension, a diffraction grating and a cylindrical lens map the wavelength onto the horizontal position (as in a conventional spectrometer) and so record a 2-D interferogram, which is the SEA TADPOLE trace.

Fig. 2 shows a measurement of a shaped pulse using SEA TADPOLE. The pulse was shaped using a 256-element liquid-crystal display pulse shaper. Fig. 2(a) shows the SEA TADPOLE trace, and it nicely illustrates that the curvature of the fringes

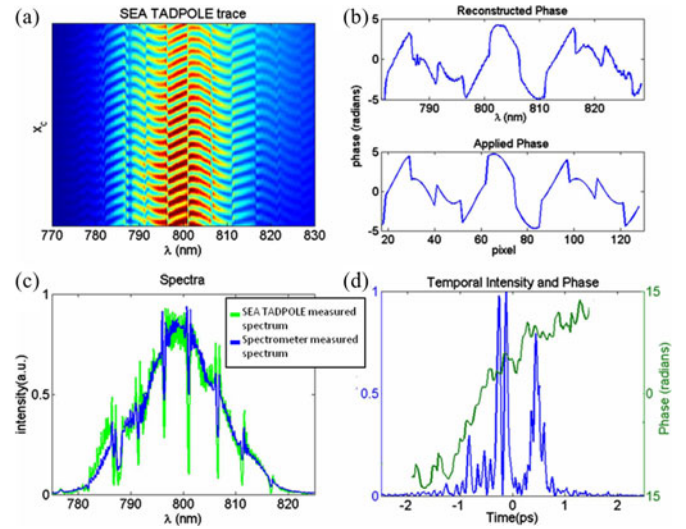


Fig. 2. (a) SEA TADPOLE trace for a shaped pulse. (b) Retrieved spectral phase compared with the phase applied to the shaper. (c) SEA TADPOLE retrieved spectrum compared with the spectrometer spectrum. (d) Retrieved temporal intensity and phase (figure reprinted from [26]).

is the phase difference between the interfering pulses. Fig. 2(b) shows the excellent agreement between the phase applied by the shaper and that measured by SEA TADPOLE. Fig. 2(c) shows the reconstructed spectrum compared with an independent spectrometer measurement. Note that the SEA TADPOLE measured spectrum is better resolved than that measured by the spectrometer (obtained simply by blocking the reference pulse). This is usually the case because SEA TADPOLE measures the not-necessarily-always-positive spectral field $E(\lambda)$ rather than the spectral intensity $E(\lambda)^2$ and so does not broaden as much when convolved with the spectrometer’s line shape [26]. Fig. 2(d) shows the reconstructed temporal field, which had a TBP of ~ 100 .

III. MEASURING THE FULL SPATIOTEMPORAL ELECTRIC FIELD OF COMPLEX PULSES

Another advantage of SEA TADPOLE is its ability to measure the full spatiotemporal electric field $E(x,y,z,t)$ of even focusing light pulses with submicrometer spatial resolution—limited spatially only by the mode size of the fiber used. Indeed, to be able to measure pulses at a focus is important because this is where most pulses are used. And because common lens aberrations can cause serious spatiotemporal distortions [28], measuring a focused pulse requires not just high spectral resolution but also high spatial resolution.

To measure a focused pulse with SEA TADPOLE, we use a fiber whose mode size is smaller than the focused spot size. Then, we measure $E(t)$ at many positions within the focus, yielding $E(x,y,z,t)$ [27]. To characterize smaller foci (with spot sizes $< 5 \mu\text{m}$), we use near-field scanning optical microscopy (NSOM) fiber probes. Fig. 3 shows the results of a SEA TADPOLE measurement of a focused pulse that reveals some interesting structure due to overfilling and aberrations in the focusing lens.

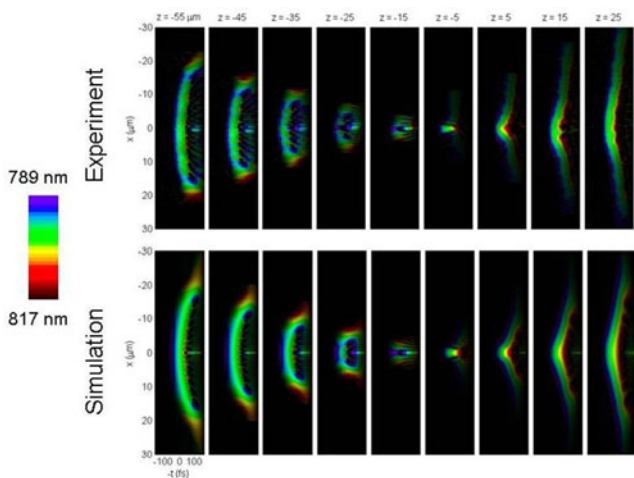


Fig. 3. xz -scanned SEA TADPOLE measurement shows the intensity and phase of a focusing pulse for an overfilled lens with an NA of 0.4. The brightness indicates the pulse intensity, and the color indicates the instantaneous frequency (indicating the pulse phase). Note the submicrometer fore-runner pulse ahead of the curved focusing pulse, predicted over a decade ago and only recently measured for the first time using SEA TADPOLE (figure reprinted from [25]).

In this measurement, the pulse was focused by a New Focus aspheric lens made of CO550 glass with a focal length of 8 mm and an aperture diameter of 8 mm; the focus had a numerical aperture (NA) of 0.44. To determine the aberrations in this lens for the simulations, we performed ray tracing using OSLO and used the lens parameters provided by New Focus.

Because this lens was designed to be used with a glass cover slip, which we did not use in our experiment, some spherical aberration is also present.

The simulation and the experiment are in good agreement. The color varies with time due to group-velocity dispersion (GVD) and also with the transverse position x due to chromatic aberration. Also, the redder colors focus later than the bluer colors, so, before the focus, the blue is at the center and the red is on the edges of the pulse.

The most striking feature in these data is the presence of the additional pulse, the so-called fore-runner pulse, which can be seen before the focus. This additional pulse results from the combination of diffraction at the edge of the lens and chromatic aberration [28], [29]. The fore-runner pulse travels faster than the main pulse front meaning that it is traveling faster than the speed of light. Again, because this additional pulse is the result of interference, it does not carry any information, so this does not violate the theory of relativity [28]. The full-width at half-maximum (FWHM) of the intensity of the additional pulse is less than $1 \mu\text{m}$. The small amount of spherical aberration present in this focus increases the intensity of the additional pulse.

IV. MEASURING BROADBAND NANOSECOND LONG PULSES USING MUD TADPOLE

It is desirable to measure even more complex pulses, in particular, broadband (20–100 nm) ns long pulses. This requires increasing the spectral resolution dramatically because, as in any spectral technique, the maximum length of a pulse that SEA TADPOLE can measure is inversely proportional to the

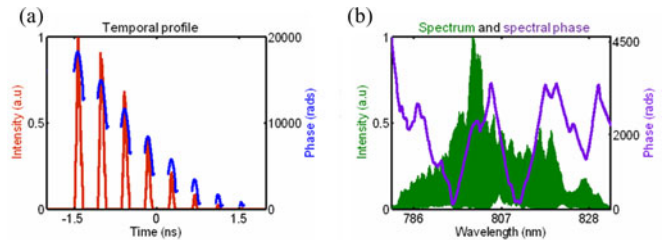


Fig. 4. (a) Temporal intensity and phase of a 3.5-ns train of pulses. The measurement shows the steadily decreasing intensities of the pulses, the expected result of the multiple reflections inside the etalon used to generate the pulse train. (b) Spectrum and spectral phase of the pulse train. This asymmetric spectrum is expected because the etalon used to generate the pulse was slightly misaligned, resulting in individual pulses in the pulse train having different temporal spacings. Additionally, the differing relative phases of the individual pulses in the pulse train also contributed to the unique spectral shape.

spectral resolution of the spectrometer used. This condition can also be expressed in terms of the temporal length of the reference pulse at the *output* of the spectrometer. A fundamental, but often overlooked, property of spectrometers is that they stretch ultrashort pulses to this value [26], [30]. This is easily understood by considering that spectrometers map a small range of frequencies, $\delta\omega$, equal to the spectral resolution, to each pixel of the detector. From the uncertainty principle, such a narrow band of frequencies can only be contained in a pulse that has a temporal duration

$$\tau_{sp} \geq \frac{1}{\delta\omega}. \quad (1)$$

Because, like other SI techniques, SEA TADPOLE requires the formation of fringes, it also requires temporal overlap of the reference and unknown pulses. Thus, it can, at best, be used to measure a pulse only τ_{sp} long.

In order to measure longer pulses, SEA TADPOLE must be outfitted with a higher resolution spectrometer, which would yield a longer τ_{sp} . Unfortunately, high-resolution spectrometers are extremely large, inconvenient, and expensive due to the proportional relationship between a spectrometer's spectral resolution and a number of grooves illuminated on the grating (and hence its, and the overall device's size).

So, instead of using a high-resolution spectrometer, we simply use a delay stage to scan the unknown pulse in time, resulting in multiple SEA TADPOLE measurements at different delays. Each SEA TADPOLE measurement retrieves a different temporal section of the electric field of the unknown pulse, where the range of each individual measurement is τ_{sp} and is much shorter than the unknown pulse duration. The retrieved spectral fields are then Fourier transformed to the time domain, yielding the retrieved section of the unknown pulse in time. Lastly, the retrieved sections are concatenated in time to reconstruct the entire unknown pulse.

We call this simple modification MUD TADPOLE [31] which stands for MULTiple Delays for Temporal Analysis by Dispersing a Pair of Light E-fields, and we have used it to measure complex pulses up to 3.5 ns in length with a bandwidth of ~ 40 nm and TBP's exceeding 65 000. Fig. 4 shows a measurement of such a pulse.

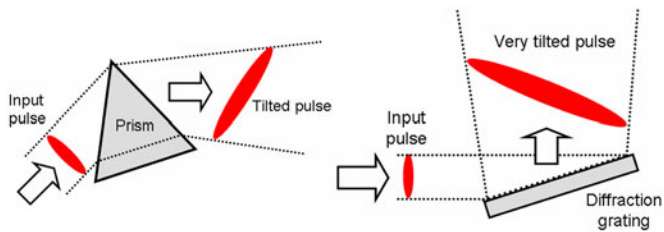


Fig. 5. Prism and a grating yield tilted pulses. While the mechanisms for generating tilt appear to be different, in both cases, it is due to their dispersion.

The train of pulses shown in Fig. 4(a) was generated by placing a mirror pair, each with a 90% partially reflecting face, after a grating pulse compressor. The compressor was used to stretch the incident pulse up to 70-ps FWHM. The mirrors were not precisely parallel, but still yielded a train of pulses at their output. The spectral bandwidth of pulses was 40-nm FWHM.

Fig. 4(b) shows the retrieved spectrum and spectral phase of the pulse train, which exhibits MUD TADPOLE's large spectral range, ~ 50 nm in this measurement. A striking feature of the spectrum is its complex shape. The unique shape is attributed to two factors. First, the two partially reflecting mirrors were deliberately aligned not to be parallel, in order to avoid back reflections back into the laser. This slight misalignment results in a different temporal spacing between the adjacent pulses in the pulse train, which corresponds to different spectral-fringe periodicities in the spectral domain. Second, the relative phase of each individual pulse in the pulse train differed, which shifted the spectral fringes due to each pulse in the train of pulses, and which served to further distort the envelope of the spectrum. Note that the spectrum is so complex that it cannot be resolved in the plot shown in Fig. 4(b).

V. SINGLE-SHOT MUD TADPOLE

Although MUD TADPOLE is the first general technique for the measurement of extremely complex pulses with fs temporal resolution, ns temporal range, pm spectral resolution, and nm spectral range, it is a scanning technique, which, by definition, requires a multitude of measurements at different delays. For this reason, it is unable to measure transient optical phenomena that vary from shot to shot, such as pulses from a true arbitrary optical waveform. To do so, it requires the generation of ns delay in a *single-shot*, another unsolved problem.

To modify MUD TADPOLE to solve this problem, we use a common spatiotemporal distortion, *pulse-front tilt*. In the 1980s, researchers realized that dispersive elements, such as prisms and gratings, yield tilted pulses (see Fig. 5). For example, a diffraction grating can generate a tilt in which one side of the pulse precedes the other by approximately its length divided by the speed of light, as can be seen in Fig. 5. And crossing two oppositely tilted pulses, generated using a high-groove-density diffraction grating, could yield a pulse, one side of which precedes the other by many ps, and overlapping them in a second harmonic generation (SHG) crystal could generate a single-shot autocorrelation of pulses tens of ps long [32].

To modify MUD TADPOLE to operate single shot, we use pulse-front tilt to replace the delay stage, providing a rather large range of delay (~ 120 ps). Fig. 6(a) shows the single-shot MUD TADPOLE setup. A diffraction grating introduces pulse-front tilt onto the spatially smooth reference pulse.

Next, a lens images the face of the diffraction grating onto the output of the imaging spectrometer. This imaging is necessary to ensure that there are no other spatiotemporal distortions in the reference pulse besides pulse-front tilt (gratings are most commonly used to generate spatial dispersion, separating a beam's colors in space, as in spectrometers, but this is achieved at a *focal* plane of a lens, whereas the colors are recombined at an *image* plane, leaving mainly pulse-front tilt, which is our requirement here).

Next, the reference pulse and the unknown pulse are interfered at a slight angle ($\sim 1^\circ$) in the x_c dimension and spectrally resolved along the opposite dimension by the spectrometer. The result is a spectrally resolved spatial interferogram (similar to SEA TADPOLE) from which both the intensity and the phase of the unknown pulse can be retrieved using a simple Fourier-retrieval algorithm [31].

Fig. 6(b) illustrates the interference of the unknown pulse and the reference pulse at the output of the imaging spectrometer. At the output of the spectrometer, the tilted reference pulse gates the unknown pulse, providing multiple delayed measurements of the unknown pulse at different positions along the x_c dimension of the detector array.

Additionally, Fig. 6 shows how the temporal range/spectral resolution in single-shot MUD TADPOLE can be increased by simply increasing the pulse-front tilt. This can be accomplished in two ways. First, a more dispersive element like an etalon could be used to further tilt the reference pulse. Or second, the already-tilted reference pulse can be tilted even further by demagnifying the image of the reference pulse on the grating or etalon. Either method can be used to increase the temporal range of single-shot MUD TADPOLE up to several ns.

Not only the temporal range/spectral resolution of the device can be adjusted easily, but the temporal resolution/spectral range of single-shot MUD TADPOLE can also be increased easily. Simply increasing the spectral range increases the temporal resolution: an easily attained spectral range of ~ 50 nm results in ~ 40 fs temporal resolution, which is 350 times faster than the fastest photodetector.

Fig. 7 shows four single-shot MUD TADPOLE measurements with a delay range of ~ 120 ps and sub-ps temporal resolution. We measured the temporal beating caused by the interference between two linear chirped pulses at variable delays. This phenomena is known as chirped pulse beating [33], and it occurs because, at each point in time, the frequency content of each pulse differs by a constant beat frequency. This beat frequency is proportional to the delay τ between the two linearly chirped pulses. The double pulse was generated by a Michelson interferometer. After pulse generation by the Michelson interferometer, we chirped the pulses with a single-grating pulse compressor [34].

The measurements in Fig. 7 simultaneously highlight the high temporal resolution and the large temporal range of MUD TADPOLE. The temporal resolution of MUD TADPOLE is

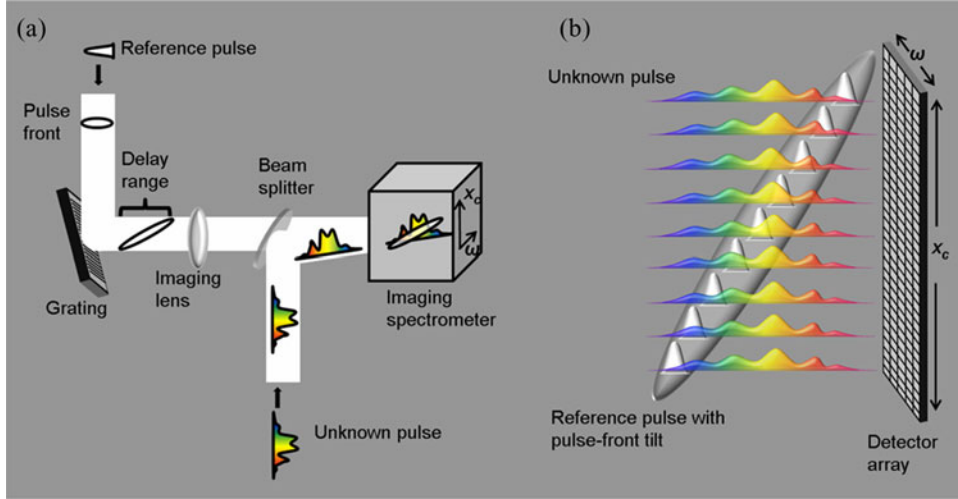


Fig. 6. (a) Experimental setup for single-shot MUD TADPOLE. The pulse front of the spatially uniform reference pulse is tilted along the horizontal dimension by a grating. The imaging lens images the plane of the grating onto the detector of the imaging spectrometer, ensuring that the only spatiotemporal coupling in the reference pulse is PFT. The unknown pulse is incident on the imaging spectrometer at a slight angle θ with respect to the reference pulse. This crossing of the two pulses results in a spatial interferogram with spatial fringes along the x_c dimension at the detector of the imaging spectrometer. (b) Gating of the unknown pulse with the tilted reference pulse at the output of the spectrometer. The spatial distribution of the unknown pulse is uniform over the entire detector, whereas the reference pulse exhibits PFT. The result is multiple delayed measurements of the unknown pulse along the x_c dimension of the detector.

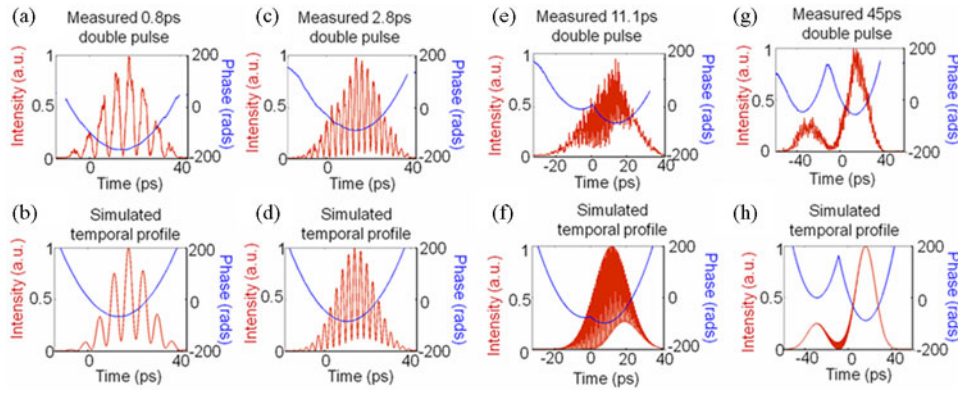


Fig. 7. Comparison of the measured and calculated temporal profiles of a chirped double pulse at variable delays. (a), (b) MUD TADPOLE retrieved and simulated temporal profile of two 21-ps linearly chirped pulses separated by 0.8 ps. (c), (d) Retrieved and simulated temporal profile after increasing the delay between pulses to 2.8 ps. (e), (f) Retrieved and simulated temporal profile after increasing the delay between pulses to 11.1 ps. At this large delay, the temporal phase develops a cusp, which MUD TADPOLE is able to retrieve. (g), (h) Retrieved and simulated temporal profile after increasing the delay between pulses to 45 ps. In this measurement, the pulses are separated by a large delay, yet there is still some temporal overlap. This results in very high frequency temporal beating.

determined by the spectral range of the spectrometer used. In this experiment, our spectrometer had a spectral range of 17 nm resulting in a temporal resolution of 130 fs. This high temporal resolution was put to good use in the measurement of the double pulse with a 11.1-ps delay shown in Fig. 7(e). The fast temporal beating, which had a temporal period of ~ 600 fs, is well resolved by MUD TADPOLE.

In addition to accurately retrieving complex temporal amplitude profiles, Fig. 7(e) and (g) shows that MUD TADPOLE also accurately measures complex phase profiles. At large delays between the two linearly chirped pulses, the temporal phase develops a cusp, which MUD TADPOLE is able to accurately retrieve.

VI. SINGLE-SHOT NANOSECOND FROG

SEA TADPOLE and MUD TADPOLE require a previously measured reference pulse. This is fine for measuring shaped

pulses and arbitrary waveforms—pulses generated from simple ultrashort laser pulses, the latter of which can also provide the appropriate reference pulse. But the vast majority of pulsed lasers emit ns pulses to begin with, and no reference pulse is available. Worse, ns pulses tend to be highly structured and variable from shot to shot, so a single-shot technique is vastly preferred.

How can we measure such pulses? Multishot FROGs have been built for pulses as long as 80 ps using long delay lines and high-resolution spectrometers [5]. Extending FROG to the ns regime requires even longer delays (meters) and higher spectral resolution (sub-pm). But to do so on a single shot is more challenging.

An etalon spectrometer can accomplish the required spectral resolution. But in order to generate a few-ns delay, it is necessary for one side of the beam to precede the other by over a meter! Using a < 1 cm-diameter beam, this corresponds to a pulse-front

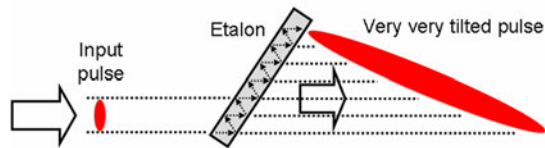


Fig. 8. Etalon's high angular dispersion yields massive pulse-front tilt. More physically, this can be seen by noting that the transmitted pulselet at the base of the etalon emerges first, while pulselets emerging from higher regions experience more delay due to their multiple reflections inside the etalon and so emerge later.

tilt (PFT) of $\sim 89.9^\circ$! How can we achieve ns delays without resorting to a meter long diffraction grating? This seems quite impractical.

On the contrary, we have recently shown that this can be done easily [35]. It is easy to show that the pulse-front tilt is proportional to the angular dispersion introduced by the component in question. And we have recently shown that an etalon, whose dispersion can be ~ 100 times that of a grating, can generate a huge pulse-front tilt (see Fig. 8). In fact, we have easily generated a pulse-front tilt of 89.9° without significantly distorting the pulse in time. Crossing two such pulses, each with opposite tilt, can achieve the required several ns delay range.

To build a simple ns FROG, we use, in addition to the etalon, a Fresnel biprism, which, as in our fs GRENOUILLE [36], conveniently generates two pulses at different angles without the need for a beam splitter and beam-recombining optics. For generating pulse-front tilt, we do not use a traditional etalon, and instead use a recently developed virtually imaged phased array (VIPA) etalon [37], which, as originally proposed, has a clear region on one edge into which the pulse is focused, yielding a highly efficient process. However, we modify it to have two clear regions: one on the top and another at the bottom for the two beams generated by the Fresnel biprism. The two beams enter the etalon and emerge overlapped and oppositely tilted by $\sim 89.9^\circ$. A lens then overlaps them at the SHG crystal. Two highly tilted, but inverted, pulses are shown as the dark red lines in Fig. 9(b). Fig. 9 shows the entire device, including the etalon spectrometer after the crystal.

Using the setup described in Fig. 9, we have made measurements of commercial ns-pulsed laser sources. Fig. 10 shows measurements of an ns Yb-fiber-amplified microdisk laser pulse [38]. In the spectral measurements shown in Fig. 10(a) and (b), we have compared the retrieved (FROG-measured) spectrum with an independently measured spectrum from a 1064-nm etalon spectrometer, and the measurements are in good agreement. Of course, FROG also yields the spectral phase and the temporal intensity and phase, not available from the spectral measurement.

For spectrally resolving the second harmonic (SH) 532-nm light, we used a custom fused silica glass-spaced VIPA etalon from CVI with a front surface reflectivity of 97% and a back surface reflectivity of 99.3% [see Fig. 9(a) and (b)]. The VIPA was round with a 1-inch diameter and a width of 10 mm, corresponding to a free spectral range of 10 pm or 10.6 GHz. The transparent gap at the bottom of the front surface was 3 mm

wide at its center, and we tilted the etalon with respect to the incoming beam by 0.9° . We experimentally found the linewidth of this etalon to be 0.13 pm (138 MHz), which we calculated by measuring the spectral fringe contrast versus delay for a double pulse from a Michelson interferometer [39]. We also used the Michelson interferometer to calibrate the FROG's frequency axis because the path-length difference can easily be measured, from which the spectral fringe spacing can be calculated. The lens for mapping wavelength onto position had a focal length of 50 cm.

The two-gap pulse-front tilt etalon [see Fig. 9(a)] was also a custom component from CVI Laser Corp. and was also glass spaced and made of fused silica. Its front and back reflectivities were 97% and 99.3%, respectively, for 1064 nm. This etalon was square with an aperture size of 30×25 mm and the two gaps on the front surface were 5×25 mm. The etalon's thickness was 10 mm, and it had a free spectral range of 38 pm (40 GHz). We used a very narrow line (\sim femtometer linewidth) cw laser to measure its linewidth and found it to be ~ 0.9 pm or 954 MHz. As a result, it had a finesse of 42. From light-travel time considerations, this results in a delay range of 8.4 ns between the two oppositely tilted pulses.

To generate the two oppositely tilted pulses, we used a Fresnel biprism with an apex angle of 160° [see Fig. 9(a) and (b)]. A $f = 120$ -mm focal-length cylindrical lens was placed at a distance slightly greater than f after the biprism to focus the two beams into the two gaps of the etalon with an incident angle of $\sim 1^\circ$ with respect to the etalon's normal. The etalon was slightly further than f away from the cylindrical lens in order to match the spacing between the two beams to the spacing between the etalon's two gaps (2 cm). This only resulted in slight loss due to clipping of the beam at the gap, and as long as the beam was diverging or converging, the angular dispersion was still generated.

Rather than the anamorphic lens used in GRENOUILLE designs [36] and shown in Fig. 9, we used two cylindrical lenses having focal lengths of 200 mm and 100 mm before the SHG crystal. This is optically equivalent to the anamorphic lens.

For the nonlinear crystal, we used a 1-cm-thick LiIO_3 crystal with an aperture size of $2 \text{ cm} \times 5 \text{ mm}$, cut to phase-match SHG at 1064 nm for collinear beams. The full crossing angle of the two tilted pulses at the SHG crystal was approximately equal to the input angle of the beams into the PFT etalon, or $\sim 2^\circ$.

The seed laser for our master oscillator fiber amplifier (MOFA) was a diode-pumped Nd:LSB microdisk laser from Standa. It emitted slightly subnanosecond pulses with $\sim 8 \mu\text{J}$ of energy and a 10-kHz repetition rate. We amplified these pulses with a one-stage fiber amplifier. The fiber was a 2m-long double-clad Yb-doped polarization-maintaining fiber with an inner-core diameter of $25 \mu\text{m}$, and an outer-core diameter of $250 \mu\text{m}$ from Nufern. We coiled the fiber to achieve single-mode operation. As the pump for the Yb-fiber amplifier, we used a diode laser from Apollo Instruments, whose wavelength was centered at 976 nm and had ~ 3 nm of bandwidth. We free-space-coupled both the pump and seed lasers into the Yb fiber, and our MOFA was very similar to the first stage of the MOFA published previously [40]. The pump and seed lasers were coupled into opposite

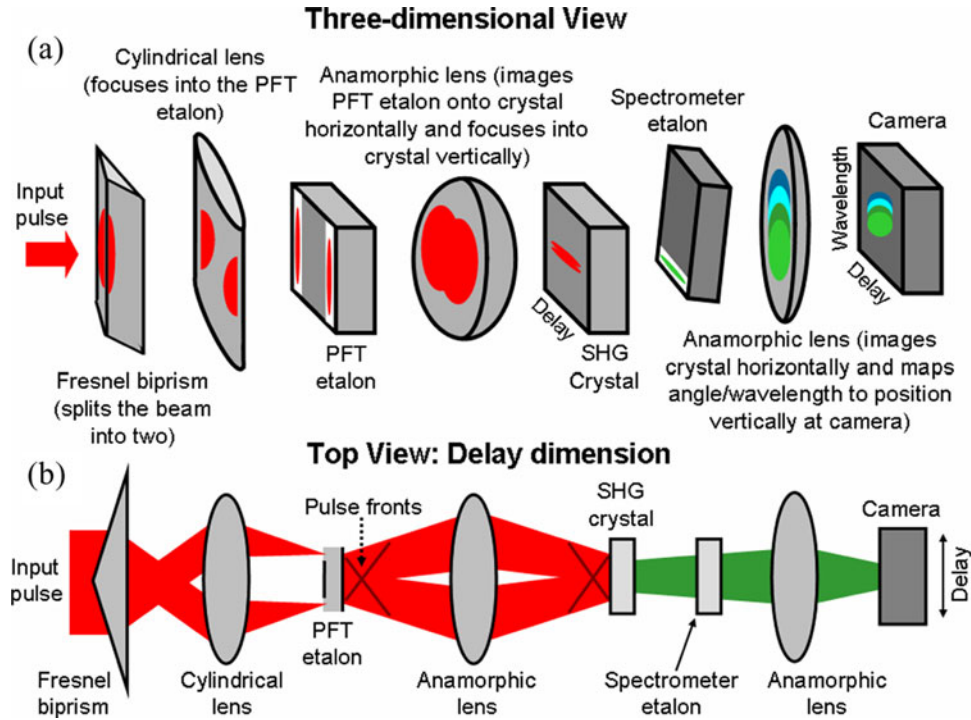


Fig. 9. (a) 3-D view of the entire ns FROG, showing the etalon spectrometer also. The SHG crystal is imaged onto a camera's horizontal dimension and spectrally resolved along the vertical dimension with an etalon spectrometer (a VIPA etalon followed by a cylindrical lens), resulting in a single-shot FROG trace at the camera. (b) Top view: the pulse to be measured is split into two crossing beams with a Fresnel biprism. A cylindrical lens focuses the two beams into the transparent gaps of the VIPA etalon. Two crossing, oppositely tilted pulse fronts emerge from the etalon. The ($\sim 89.9^\circ$) tilted pulse fronts are imaged onto the SHG crystal to produce the pulse's autocorrelation. A slit at the focal plane of the first imaging lens removes the higher orders from the etalon.

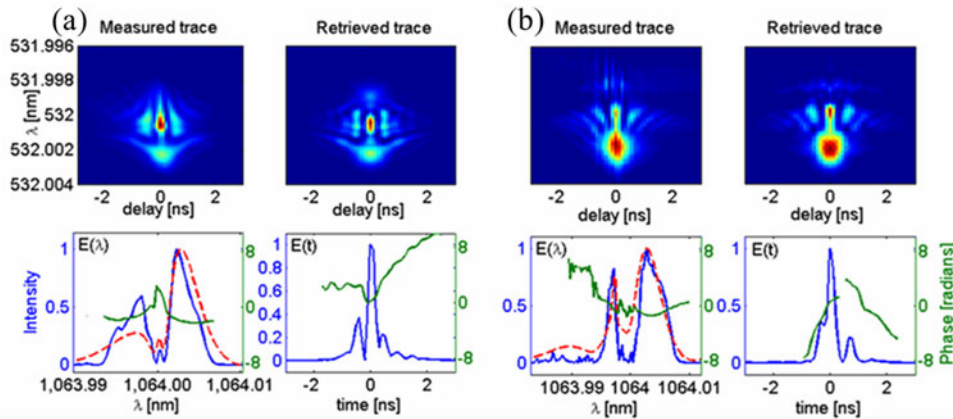


Fig. 10. Nanosecond FROG measurements of Yb-fiber-amplified pulses from a microchip laser. Top: measured and retrieved FROG traces (spectrograms) for two different pulses (different amounts of amplification). Bottom: the retrieved spectral and temporal intensities and phases. The red line shows an independent etalon spectrometer measurement of the spectrum. Note the agreement with the FROG-measured spectrum and the better spectral resolution of the FROG measurement.

ends of the fiber to reduce the nonlinearities. The pulses shown in Fig. 10 (a) and (b) were amplified by $12\times$ and $15\times$, resulting in an average power of 170 mW and 213 mW, respectively, for the amplified seed laser. This required 2 W and 2.8 W of pump power, respectively, not accounting for coupling losses and loss at the dichroic mirror.

Because the tilt of the pulse front can be varied, the delay range and resolution can be chosen to cover a wide range of pulse lengths up to tens of ns or longer. Also, the spectral range and minimum resolvable spectral features of the FROG

are determined by the SH etalon spectrometer. Finally, note that, in both of our preliminary measurements, the spectral resolution of the FROG was better than that of our etalon spectrometer even though it also used a similar etalon spectrometer. Indeed, FROG measurements usually prove more reliable at higher resolution, especially for complex spectra. As a result, even longer pulses could be measured using our ns FROG because its use of a long delay range to obtain redundant spectral information could help to allow it to achieve ultrahigh spectral resolution.

In any case, the single-shot ns FROG is the first practical device for measuring the complete intensity and phase versus time (and frequency) of the most commonly used laser pulses, \sim ns in length. It naturally operates single shot, so it can also see any fluctuations in the pulse shape from shot to shot in a train. It is easy to use, requiring no alignment, and it is entirely passive, requiring no expensive and fragile electronics; its only electronic component is a common, few-hundred-dollar <1 megapixel camera. It uses the same commercially available real-time FROG software that has proven successful for retrieving fs pulses; all that is necessary is a change of scale in its parameters. In short, we believe that this simple device could prove as essential an accessory in ns laser laboratories as fs FROG (GRENOUILLE) has become in fs laser laboratories.

VII. CONCLUSION

We have reviewed three recent extensions of ultrashort pulse metrology that completely measure the electric field of both complex shaped pulses (in time and space) and ns long pulses directly from ns lasers when a reference pulse is unavailable. We believe that the long temporal range, or equivalently, the high spectral resolution of these methods, coupled with their ability to measure complex pulses, provides a substantial improvement to the field of pulsed waveform metrology.

ACKNOWLEDGMENT

The authors acknowledge support from DARPA grant #FA8650-09-C-9733 and help from Rick Toman of CVI Laser Corporation with the custom etalons. The views, opinions, and/or findings contained in this paper are those of the authors and should not be interpreted as representing the official views or policies, either expressed or implied, of the Defense Advanced Research Projects Agency or the Department of Defense.

REFERENCES

- [1] J. A. Giordmaine, P. M. Rentzepis, S. L. Shapiro, and K. W. Wecht, "Two-photon excitation of fluorescence by picosecond light pulses," *Appl. Phys. Lett.*, vol. 11, pp. 216–218, 1967.
- [2] K. L. Sala, G. A. Kenney-Wallace, and G. E. Hall, "CW autocorrelation measurements of picosecond laser pulses," *IEEE J. Quantum Electron.*, vol. 16, no. 9, pp. 990–996, Sep. 1980.
- [3] J. Peatross and A. Rundquist, "Temporal decorrelation of short laser pulses," *J. Opt. Soc. Amer. B, Opt. Phys.*, vol. 15, pp. 216–222, 1998.
- [4] R. Trebino, *Frequency-Resolved Optical Gating: The Measurement of Ultrashort Laser Pulses*. Boston: Kluwer, 2002.
- [5] H. Fuchs, D. Woll, T. Ulm, and J. A. L'Huillier, "High resolution FROG system for the characterization of ps laser pulses," *Appl. Phys. B (Lasers Opt.)*, vol. 88, pp. 393–96, 2007.
- [6] J. M. Dudley, C. Finot, D. J. Richardson, and G. Millot, "Self-similarity in ultrafast nonlinear optics," *Nat. Phys.*, vol. 3, pp. 597–603, 2007.
- [7] M. E. Fermann, B. C. Thomsen, V. I. Kruglov, J. M. Dudley, and J. D. Harvey, "Propagation and compression of high power parabolic pulses generated in a high gain Yb:doped fibre amplifier," presented at the Eur. Conf. Lasers and Electro-Optics, Nice, France, Sep. 10–15, 2000.
- [8] C. Finot, G. Millot, C. Billet, and J. M. Dudley, "Experimental generation of parabolic pulses via Raman amplification in optical fiber," *Opt. Exp.*, vol. 11, pp. 1547–1552, 2003.
- [9] J. Cohen, D. Lee, V. Chauhan, P. Vaughan, and R. Trebino, "Highly simplified device for measuring the intensity and phase of picosecond pulses," *Opt. Exp.*, vol. 18, pp. 17484–17497, 2010.
- [10] X. Gu, L. Xu, M. Kimmel, E. Zeek, P. O'Shea, A. P. Shreenath, R. Trebino, and R. S. Windeler, "Frequency-resolved optical gating and single-shot spectral measurements reveal fine structure in microstructure-fiber continuum," *Opt. Lett.*, vol. 27, pp. 1174–1176, 2002.
- [11] M. A. Foster, S. Salem, D. F. Geraghty, A. Turner-Foster, M. Lipson, and A. L. Gaeta, "Silicon-chip-based ultrafast optical oscilloscope," *Nature*, vol. 456, pp. 81–84, 2008.
- [12] D. H. Broaddus, M. A. Foster, O. Kuzucu, A. C. Turner-Foster, K. W. Koch, M. Lipson, and A. L. Gaeta, "Temporal-imaging system with simple external-clock triggering," *Opt. Exp.*, vol. 18, pp. 14262–14269, 2010.
- [13] M. Skold, M. Westlund, H. Sunnerud, and P. A. Andrekson, "All-optical waveform sampling in high-speed optical communication systems using advanced modulation formats," *J. Lightw. Technol.*, vol. 27, pp. 3662–3671, 2009.
- [14] M. Vampouille, A. Barthélémy, B. Colombeau, and C. Froely, "Observation et applications des modulations de fréquence dans les fibres unimodales," *J. Opt. (Paris)*, vol. 15, pp. 385–390, 1984.
- [15] E. J. R. Kelleher, J. C. Travers, E. P. Ippen, Z. Sun, A. C. Ferrari, S. V. Popov, and J. R. Taylor, "Generation and direct measurement of giant chirp in a passively mode-locked laser," *Opt. Lett.*, vol. 34, pp. 3526–3528, 2009.
- [16] C. Dorrer and I. Kang, "Linear self-referencing techniques for short-optical-pulse characterization," *J. Opt. Soc. Amer. B*, vol. 25, pp. A1–A12, 2008.
- [17] I. A. Walmsley and C. Dorrer, "Characterization of ultrashort electromagnetic pulses," *Adv. Opt. Photon.*, vol. 1, pp. 308–437, 2009.
- [18] C. Froehly, A. Lacourt, and J. C. Vienot, "Time impulse response and time frequency response of optical pupils," *Nouvelle Revue D'Optique*, vol. 4, pp. 183–196, 1973.
- [19] D. N. Fittinghoff, J. L. Bowie, J. N. Sweetser, R. T. Jennings, M. A. Krumbügel, K. W. DeLong, R. Trebino, and I. A. Walmsley, "Measurement of the intensity and phase of ultraweak, ultrashort laser pulse," *Opt. Lett.*, vol. 21, pp. 884–886, 1996.
- [20] P. Bownan, P. Gabolde, A. Shreenath, K. McGresham, and R. Trebino, "Crossed-beam spectral interferometry: A simple, high-spectral-resolution method for completely characterizing complex ultrashort pulses in real time," *Opt. Exp.*, vol. 14, pp. 11892–11900, 2006.
- [21] M. H. Asghari, Y. Park, and J. Azaña, "Complex-field measurement of ultrafast dynamic optical waveforms based on real-time spectral interferometry," *Opt. Exp.*, vol. 18, pp. 16526–16538, 2010.
- [22] N. K. Fontaine, R. P. Scott, L. Zhou, F. M. Soares, J. P. Heritage, and S. J. B. Yoo, "Real-time full-field arbitrary optical waveform measurement," *Nat. Photon.*, vol. 4, pp. 248–254, 2010.
- [23] N. K. Fontaine, R. P. Scott, J. P. Heritage, and S. J. B. Yoo, "Near quantum-limited, single-shot coherent arbitrary optical waveform measurements," *Opt. Exp.*, vol. 17, pp. 12332–12344, 2009.
- [24] C. Dorrer, M. Joffre, L. Jean-Pierre, and N. Belabas, "Spectral resolution and sampling issues in Fourier-transform spectral interferometry," *J. Opt. Soc. Amer. B*, vol. 17, pp. 1790–1802, 2000.
- [25] P. Bownan, U. Fuchs, R. Trebino, and U. D. Zeitner, "Measuring the spatiotemporal electric field of tightly focused ultrashort pulses with sub-micron spatial resolution," *Opt. Exp.*, vol. 16, pp. 13663–13675, 2008.
- [26] P. Bownan, P. Gabolde, M. A. Coughlan, R. Trebino, and R. J. Levis, "Measuring the spatiotemporal electric field of ultrashort pulses with high spatial and spectral resolution," *J. Opt. Soc. Amer. B*, vol. 25, pp. A81–A92, 2008.
- [27] P. Bownan, P. Gabolde, and R. Trebino, "Directly measuring the spatiotemporal electric field of focusing ultrashort pulses," *Opt. Exp.*, vol. 15, pp. 10219–10230, 2007.
- [28] U. Fuchs, U. D. Zeitner, and A. Tuennermann, "Ultra-short pulse propagation in complex optical systems," *Opt. Exp.*, vol. 13, pp. 3852–3861, 2005.
- [29] Z. Bor and Z. L. Horváth, "Distortion of femtosecond pulses in lenses. Wave optical description," *Opt. Commun.*, vol. 94, pp. 249–258, 1992.
- [30] B. Rubin and R. M. Herman, "Monochromators as light stretchers," *Amer. J. Phys.*, vol. 49, p. 868, 1981.
- [31] J. Cohen, P. Bownan, V. Chauhan, and R. Trebino, "Measuring temporally complex ultrashort pulses using multiple-delay crossed-beam spectral interferometry," *Opt. Exp.*, vol. 18, pp. 6583–6597, 2010.
- [32] R. Wyatt and E. E. Marinero, "Versatile Single-shot background-free pulse duration measurement technique for pulses of subnanosecond to picosecond duration," *Appl. Phys.*, vol. 25, pp. 297–301, 1981.
- [33] A. S. Welington and D. H. Auston, "Novel sources and detectors for coherent tunable narrow-band terahertz radiation in free space," *J. Opt. Soc. Amer. B*, vol. 13, pp. 2783–2791, 1996.

- [34] V. Chauhan, P. Bowlan, J. Cohen, and R. Trebino, "Single-diffraction-grating and grism pulse compressors," *J. Opt. Soc. Amer. B*, vol. 27, pp. 619–624, 2010.
- [35] P. Bowlan and R. Trebino, "Extreme pulse-front tilt from an etalon," *J. Opt. Soc. Amer. B*, vol. 27, pp. 2322–2327, 2010.
- [36] P. O'Shea, M. Kimmel, X. Gu, and R. Trebino, "Highly simplified device for ultrashort-pulse measurement," *Opt. Lett.*, vol. 26, pp. 932–934, 2001.
- [37] M. Shirasaki, "Large angular dispersion by a virtually imaged phased array and its application to a wavelength demultiplexer," *Opt. Lett.*, vol. 21, pp. 366–368, 1996.
- [38] P. Bowlan and R. Trebino, "Complete single-shot measurement of arbitrary nanosecond laser pulses in time," *Opt. Exp.*, vol. 19, pp. 1367–1377, 2010.
- [39] C. Dorrer, "Influence of the calibration of the detector on spectral interferometry," *J. Opt. Soc. Amer. B*, vol. 16, pp. 1160–1168, 1999.
- [40] F. Di Teodoro and C. D. Brooks, "1.1 MW peak-power, 7 W average-power, high-spectral-brightness, diffraction-limited pulses from a photonic crystal fiber amplifier," *Opt. Lett.*, vol. 30, pp. 2694–2696, 2005.



Jacob Cohen received the B.S. degree in physics from the University of Texas, Austin, in 2002, the Master's degree in applied physics from the University of Maryland, Baltimore County, Baltimore, in 2005, and the Ph.D. degree in physics from the Georgia Institute of Technology, Atlanta, in 2010 under the supervision of Prof. R. Trebino.

Since November 2010, he has been with ASML, Eindhoven, Netherlands. His research focuses on the measurement of ultrashort pulses with high spectral resolution and high temporal resolution.



Pamela Bowlan received the Ph.D. degree in physics from Rick Trebino's Group at the Georgia Institute of Technology, Atlanta, in 2009. The focus of her Ph.D. research was the characterization of ultrashort pulses that are complex in time and/or space such as focused or shaped pulses.

During the following year, she was a Swamp Optics Research Fellow, and worked to extend the FROG technique to measure nanosecond pulses. In the summer of 2010, she began working as a Postdoctoral Scholar at the Max-Born-Institute, Berlin, Germany,

for Nonlinear Optics and Short Pulse Spectroscopy in the group of Thomas Elsaesser.



Rick Trebino (S'79–M'83) was born in Boston, MA, on January 18, 1954. He received the B.A. degree from Harvard University, Cambridge, MA, in 1977, and the Ph.D. degree from Stanford University, Palo Alto, CA, in 1983. His dissertation research involved the development of a technique for the measurement of ultrafast events in the frequency domain using long-pulse lasers by creating moving gratings. He continued this research during a three-year term as a Physical Sciences Research Associate at Stanford.

In 1986, he moved to Sandia National Laboratories, Livermore, CA, where he invented FROG, the first technique for the measurement of the intensity and phase of ultrashort laser pulses. In 1998, he became the Georgia Research Alliance-Eminent Scholar Chair of Ultrafast Optical Physics at the Georgia Institute of Technology, Atlanta, where he currently studies ultrafast optics and applications. His interests include adventure travel, archaeology, and primitive art.

Dr. Trebino has received several prizes, including the SPIE's Edgerton Prize. He was an IEEE Lasers and Electro-Optics Society Distinguished Lecturer, and is a Fellow of the Optical Society of America, the American Physical Society, and the American Association for the Advancement of Science.